**Iraqi Geological Journal**

Journal homepage: https://www.igj-iraq.org

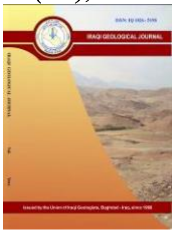

# Spatial Modeling of Groundwater Quality Parameters on Mosul's Left Bank

**Mohammed F. Khattab [1,*], Hazim J. Mahmood [2] and Eman S. Al-Sarraj [3]**

[1] Center of Remote Sensing, University of Mosul, Mosul, Iraq
[2] College of Environmental Science and Technology, University of Mosul, Mosul, Iraq
[3] Department of Pharmacy, Al-Noor University College, Mosul, Iraq
* **Correspondence**: mohamed76@uomosul.edu.iq

Received: 22 June 2022

Accepted: 18 December 2022

Published: 30 April 2023

## Abstract

Spatial distribution of groundwater quality is one of the issues that are urgently requested from both the people and decision-makers, especially during the deficiency of water network supply. This work included creating spatial groundwater quality maps on Mosul's left bank. The water quality studied parameters were pH, EC, TDS, $Ca^{2+}$, $Mg^{2+}$, $K^{+}$, $Na^{+}$, $SO_4^{2-}$, $HCO_3^-$, $NO_3^-$, $Cl^-$ and other chemical water quality parameters as well as heterotrophic bacteria. A statistical investigation has been done to evaluate the relationship between these parameters. An inverse distance weighted interpolation model was used to give these parameters a better geographical distribution pattern. The visual groundwater quality models gave an overview of this water source's environmental reality and possible pollution points. The results of this work could be employed as an effective tool in the field of planning and environmental protection of water resources in Mosul City because there is polluted groundwater on the eastern side of Mosul which is polluted by septic tanks and the sewage system

**Keywords:** Spatial modeling; Groundwater quality; Spatial distribution; Mosul; groundwater quality maps

## 1. Introduction

Water resources over the world have been suffering from quality degradation as a result of population growth with accompanying activities and climate change (Dandge and Patil, 2021). Groundwater is more sensitive to this challenge, not because it's a sustainable source of water but as a result of being the only accessible source of water supply during crises (Khattab et al., 2021). This entails knowledge of the processes and factors influencing and controlling groundwater quality to maintain this resource (Kale et al., 2020). Spatial analysis and representation of the required water quality parameters is a powerful tool that can be used effectively to understand the groundwater system and hence provide a successful management plan for these resources (Adnan and Iqbal, 2014; Barmakova et al., 2022; Dandge and Patil, 2021; Pande and Moharir, 2018). Recently, GIS interpolation functions have been widely used in several water resource hydrological aspects (Ditthakit et al., 2021; Zhou and Li, 2020). The inverse distance weighting (IDW) method represents one of the most potent spatial interpolation techniques compared to others (Khattab and Merkel, 2012). Where this method is very elastic for determining the direction of interpolation and setting up barriers.

The objective of this work is to discover the spatial distribution of groundwater quality parameters by creating maps on the eastern side of Mosul city. These parameters comprised pH, EC, TDS, $Ca^{2+}$,

DOI: 10.46717/igj.56.1D.5ms-2023-4-14

$Mg^{2+}$, $K^+$, $Na^+$, $SO_4^{2-}$, $HCO_3^-$, $NO_3^-$, $Cl^-$ as well as Heterotrophic Bacteria. The IDW interpolation technique was applied to create these maps by adjusting models to minimize estimation error. The results of this work could be employed as an effective tool in the field of planning and environmental protection of the water resources of Mosul City.

## 2. Materials and Methods

### 2.1. Geographic and Hydrological Setting

The research area is about 466 kilometers northwest of Baghdad (Iraq's capital) (Fig. 1). The coordinates for the area of interest are 36º 25′ 30″ and 36º 18′ 00″ latitude and 43º 06′ 00″ and 43º 14′ 30″ longitudes (AtlasWorld, 2019). Mosul city is divided into two distinct banks by the Tigris River: the left (eastern) and right (western) banks. The left bank is about 140 square kilometers in area, with 51 residential quarters and a population of more than 750.000 people (UN-Habitat, 2016).

The climate region of Mosul City is semi-arid which is hot during the summer and arid, while during winter is partly overcast and cold (Climate-Data.Org, 2019;WeatherSpark, 2019). The rainfall is occasionally during the winter season. The average annual rainfall from the period between 1980 to 2005 was about 370.4 mm. The Tigris River reaches the city from the north and flows south, with an average yearly discharge ranging from 270 to 1371 m3/sec, depending on the amount of snow and rain that falls on the river basin (Khattab and Merkel, 2015; Saleh, 2010).

The study area includes rocks from the Miocene to the Recent Deposits. The oldest rock outcrops in the study area are the Fatha Formation (Middle Miocene), which consists of claystone, marl, limestone, anhydrite, and gypsum strata. The formation is mostly covered by the Injana Formation (Upper Miocene) to the north of the area of interest. The latter formation consists of claystone, siltstone, and sandstone. River terraces, which represent Quaternary deposits, can be seen to the west near the river, and consist of conglomerate and gravel with sand and silt lenses. Residual soil is the main deposit that covers the majority of the study area and is consisted of loamy and sandy soil (Sissakian, 1995). After all, the banks of the Tigris and Al-Khoser rivers are surrounded by flood plain deposits (Al-Jiburi and Al-Basrawi, 2015)

### 2.2. Data Collection and Analysis

Thirteen water samples were collected from wells that were dug to alleviate the scarcity of water during ISIS's occupation of Mosul and the subsequent military operations to liberate the city. The wells were selected to cover the majority of the neighborhoods on the city's left side (Fig. 1). The selected wells ranged in depth from 12 to 60 m. GPS was used to pinpoint the locations of the wells. Electrical conductivity, T, pH, and TDS were measured in the field with the standard procedures using portable device (Sundaram, 2009)

The major ions ($Mg^{2+}$, $Ca^{2+}$, $K^+$, $Na^+$, and $SO_4^{2-}$) were measured using an ICP-MS after the samples were acidified with ultrapure $HNO_3$ and filtered through a 0.2 µm membrane filter. The concentrations of $NO_3^-$, $Cl^-$ ,and $HCO_3^-$ were determined without acidification using titration methods for $HCO_3^-$ and $Cl^-$, and a UV spectrophotometer for $NO_3^-$. The TPC bacteria analysis was carried out in accordance with standard procedures (APHA, 2005). The ICP-MS analysis was carried out at the TU Bergakademie Freiberg in Germany. $NO_3^-$, $Cl^-$, $HCO_3^-$, and TPC Bacteria tests were conducted at the College of Science, University of Mosul. The pH, EC, and TDS were collected in the field. The results of field and laboratory work have been statistically processed to provide a better understanding of the relationships between environmental parameters (Khattab et al., 2020). The root mean square error, direction, distance and mean center have been adjusted to select the best model interpolation for water quality data using

ArcGIS 10.6. Spatial model by inverse distance weight was used to interpolate the spatial distribution of groundwater quality parameters.

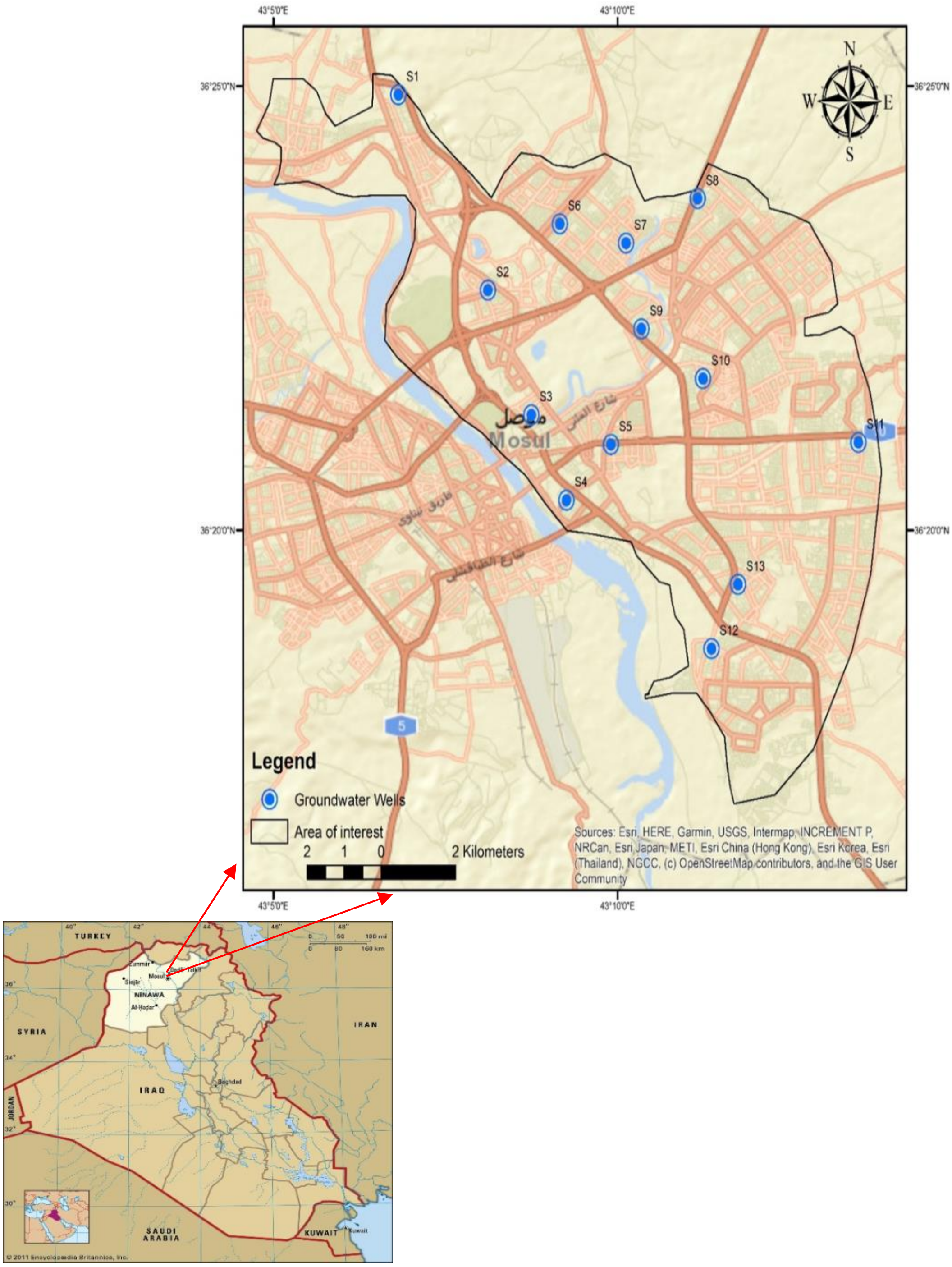


**Fig.1:** Study area map with sampling locations

## 3. Results and Discussion

### 3.1. Water Quality Data

Table 1 presents the results of the current study's field and laboratory analyses of the samples. These results included pH, EC, TDS, $Ca^{2+}$, $Mg^{2+}$, $K^{+}$, $Na^{+}$, $SO_4^{2-}$, $NO_3^{-}$, $HCO_{3-}$ $Cl^{-}$ and TPC values.

**Table 1.** Laboratory and field analysis of groundwater samples

| Sample | pH | EC | TDS | Cations (PPM) | | | | Anions (PPM) | | | | Bacteria |
|---|---|---|---|---|---|---|---|---|---|---|---|---|
| | | (µs/cm)) | (ppm) | $Ca^{2+}$ | $Mg^{2+}$ | $Na^{+}$ | $K^{+}$ | $HCO_3^-$ | $SO_4^{2-}$ | $Cl^-$ | $NO_3^-$ | TPC |
| **S1M** | 6.98 | 2922 | 2480 | 597.6 | 99.3 | 87.8 | 4.0 | 375.2 | 1648.7 | 70.0 | 20.5 | $6*10^3$ |
| **S2M** | 7.14 | 2116 | 1756 | 226.3 | 133.7 | 108.1 | 11.5 | 402.5 | 976.1 | 46.0 | 4.8 | $4*10^3$ |
| **S3M** | 7.37 | 1310 | 1097 | 136.5 | 66.2 | 80.4 | 23.0 | 345.3 | 429.2 | 56.0 | 9.4 | $4*10^3$ |
| **S4M** | 7.19 | 1814 | 1505 | 226.2 | 107.2 | 78.7 | 9.0 | 362.1 | 814.2 | 66.0 | 7.7 | $4*10^3$ |
| **S5M** | 7.04 | 2721 | 2312 | 468.5 | 165.0 | 46.1 | 25.2 | 512.4 | 1412.5 | 76.0 | 0.7 | $4*10^3$ |
| **S6M** | 7.22 | 1612 | 1328 | 162.5 | 105.8 | 83.0 | 1.8 | 375.8 | 522.0 | 100.4 | 46.0 | $7*10^3$ |
| **S7M** | 7.19 | 1814 | 1505 | 198.4 | 141.8 | 56.0 | 1.4 | 429.3 | 702.8 | 76.0 | 22.5 | $6*10^3$ |
| **S8M** | 7.15 | 2015 | 1673 | 172.5 | 143.3 | 164.4 | 1.6 | 479.8 | 728.8 | 136.0 | 42.7 | $6*10^3$ |
| **S9M** | 7.34 | 3829 | 3214 | 547.2 | 197.6 | 290.1 | 5.3 | 457.4 | 2154.7 | 185.9 | 10.2 | $9*10^3$ |
| **S10M** | 7.19 | 1612 | 1330 | 191.0 | 100.5 | 88.9 | 1.4 | 387.2 | 556.9 | 66.0 | 35.2 | $7*10^3$ |
| **S11M** | 7.1 | 1008 | 834 | 110.4 | 51.7 | 78.7 | 1.7 | 323.2 | 187.2 | 78.0 | 51.8 | $7*10^3$ |
| **S12M** | 7.47 | 1310 | 1123 | 232.5 | 78.0 | 31.8 | 1.2 | 354.5 | 598.2 | 26.0 | 14.2 | $4*10^3$ |
| **S13M** | 7.2 | 1914 | 1589 | 287.8 | 81.3 | 84.7 | 2.1 | 400.2 | 676.4 | 94.0 | 52.8 | $3*10^3$ |

### 3.2. Statistical Investigation

This section provides a statistical descriptive review of groundwater quality data (Table 2). The minimum, maximum, standard deviation, mean, and standard error for the water quality parameters investigated have all been calculated. Mean, Std. Dev. and Std. Error for EC, TDS, $SO_4^{2-}$, and TPC indicate that values of these parameters are more range out of the mean. The correlation coefficient matrix for groundwater parameters of Mosul City's left bank is shown in Table 3.

**Table 2**. Statistical overview for groundwater samples

| Variables | Min. | Max. | Mean | Std. Dev. | Std. Error |
|---|---|---|---|---|---|
| pH | 7.0 | 7.5 | 7.19 | 0.133 | 0.036 |
| EC | 1008.0 | 3829.0 | 1999.7 | 677.09 | 212.4 |
| TDS | 834.0 | 3214.0 | 1672.7 | 650.60 | 180.4 |
| $Ca^{2+}$ | 110.4 | 597.6 | 273.6 | 159.33 | 44.1 |
| $Mg^{2+}$ | 51.7 | 197.6 | 113.1 | 41.47 | 11.5 |
| $Na^{+}$ | 31.8 | 290.1 | 98.3 | 65.76 | 18.2 |
| $K^{+}$ | 1.2 | 25.2 | 6.8 | 8.30 | 2.30 |
| $HCO_3^-$ | 323.2 | 512.4 | 400.3 | 55.46 | 15.38 |
| $SO_4^{2-}$ | 187.2 | 2154.7 | 877.5 | 548.0 | 151.98 |
| $Cl^-$ | 26.0 | 185.9 | 82.7 | 40.86 | 11.33 |
| $NO_3^-$ | 0.7 | 52.8 | 24.5 | 18.81 | 5.21 |
| TPC | $3*10^3$ | $9*10^3$ | 5461.5 | 1761.40 | 488.5 |

The strong positive correlation between $Ca^{2+}$ and $SO_4^{2-}$, both of which have a strong correlation with TDS and EC (Table 3), indicates that the process of dissolving gypsum is the most influential factor in the supply of ions to groundwater, which is one of the consequences of gypsum's widespread in the study area's aquifer rocks (Khattab et al., 2021). The strong correlation between $Na^+$and $Cl^-$ suggests that halite is dissolving. The positive correlation (0.86) between $Mg^{2+}$ and $HCO_3^-$ indicates the interaction between water and magnesium carbonate (Saha et al. 2019).

### 3.3. Spatial Interpolation Model

Fig. 2 depicts the spatial distribution of groundwater quality parameters in the samples collected from Mosul's left bank. These spatial models were created by ArcGIS using the inverse distance weight interpolation technique

**Table 3.** Correlation coefficient between water quality parameters

| | pH | EC | TDS | $Ca^{2+}$ | $Mg^{2+}$ | $Na^{+}$ | $K^{+}$ | $HCO_3^-$ | $SO_4^{2-}$ | $Cl^-$ | $NO_3^-$ | TPC |
|---|---|---|---|---|---|---|---|---|---|---|---|---|
| pH | 1 | | | | | | | | | | | |
| EC | -0.22 | 1.00 | | | | | | | | | | |
| TDS | -0.22 | 1.00 | 1.00 | | | | | | | | | |
| $Ca^{2+}$ | -0.29 | 0.90 | 0.91 | 1.00 | | | | | | | | |
| $Mg^{2+}$ | -0.12 | 0.80 | 0.80 | 0.53 | 1.00 | | | | | | | |
| $Na^{+}$ | 0.14 | 0.67 | 0.66 | 0.37 | 0.60 | 1.00 | | | | | | |
| $K^{+}$ | -0.06 | 0.15 | 0.16 | 0.17 | 0.16 | -0.15 | 1.00 | | | | | |
| $HCO_3^-$ | -0.26 | 0.64 | 0.64 | 0.44 | 0.86 | 0.37 | 0.25 | 1.00 | | | | |
| $SO_4^{2-}$ | -0.18 | 0.98 | 0.99 | 0.93 | 0.75 | 0.60 | 0.18 | 0.56 | 1.00 | | | |
| $Cl^-$ | -0.01 | 0.62 | 0.61 | 0.34 | 0.62 | 0.87 | -0.21 | 0.52 | 0.51 | 1.00 | | |
| $NO_3^-$ | -0.15 | -0.40 | -0.41 | -0.41 | -0.43 | -0.03 | -0.66 | -0.23 | -0.51 | 0.23 | 1.00 | |
| TPC | -0.04 | 0.34 | 0.33 | 0.17 | 0.34 | 0.62 | -0.44 | 0.09 | 0.29 | 0.65 | 0.26 | 1.00 |

The value of the interpolation point in this technique has an effect on the interpolation point by weight (Liu et al., 2021). These predicted models for groundwater quality parameters have been adjusted to minimise estimation error. The mean and root mean square (RMS) for each predicted spatial value have been calculated (Table 4). The pH values ranged from 6.98 to 7.46, with the highest values found in the residual soil aquifer near the Tigris River and the lowest in the Fatha aquifers. The decrease in pH value indicated the absence of calcite in the water (Saha et al., 2019). Ca concentrations are higher in the north and middle of the left Mosul bank due to the presence of water within the gypsum rocks in these areas. Mg concentration increases westward, with a higher value in the middle area of interest. TDS, $SO_4^{2-}$, and EC all follow the same spatial pattern (Fig. 2). The higher values were found in the north and middle of the left Mosul bank. This is due to the direct relationship between electrical conductivity values and sulphate rocks (Guinea et al., 2012). $Na^+$ spatial model values range from 31.8 to 289.9. A high $Na^+$ value could indicate pollution from both point and non-point sources (Panno et al., 2006). This distribution pattern is comparable to the $Cl^-$ spatial model. The $K^+$ map shows that the majority of the study area has low values, except for the area near the Tigris River within the Injana aquifer. Potassium can enter groundwater through fertiliser use, animal or waste product breakdown, and clay mineral decomposition (Saha et al., 2019). $NO_3^-$ and total plate count of bacteria suggest that groundwater in the east part of the study area is contaminated by septic tanks and sewerage system leaks (Satyaji Rao et al., 2012). The $NO_3^-$ spatial value model had a range of 0.73 to 52.7 ppm. $HCO_3^-$ has the same spatial distribution as Mg, indicating that dolomite is the main source of these ions in the groundwater of the study area (Zhang et al., 2020). TPC spatial distribution shows that pollution increases away from the river, which could be due to the fact that neighborhoods near the river are less densely populated than those farther away from the river and have a better sewage system.

**Table 4.** RMSE and Mean error in Inverse distance weight method

| Variables | Mean Error | R.M.S. Error |
|---|---|---|
| pH | 0.02 | 0.14 |
| EC | 314.7 | 927.5 |
| TDS | 268.4 | 789.6 |
| $Ca^{2+}$ | 66.4 | 196.3 |
| $Mg^{2+}$ | 19.9 | 44.9 |
| $Na^{+}$ | 48.1 | 94.1 |
| $K^{+}$ | 9.5 | 12.2 |
| $HCO_3^-$ | 15.32 | 62.8 |
| $SO_4^{2-}$ | 319.3 | 713.7 |
| $Cl^-$ | 21.9 | 50.8 |
| $NO_3^-$ | 10.0 | 22.3 |
| TPC | 507.3 | 1553.6 |

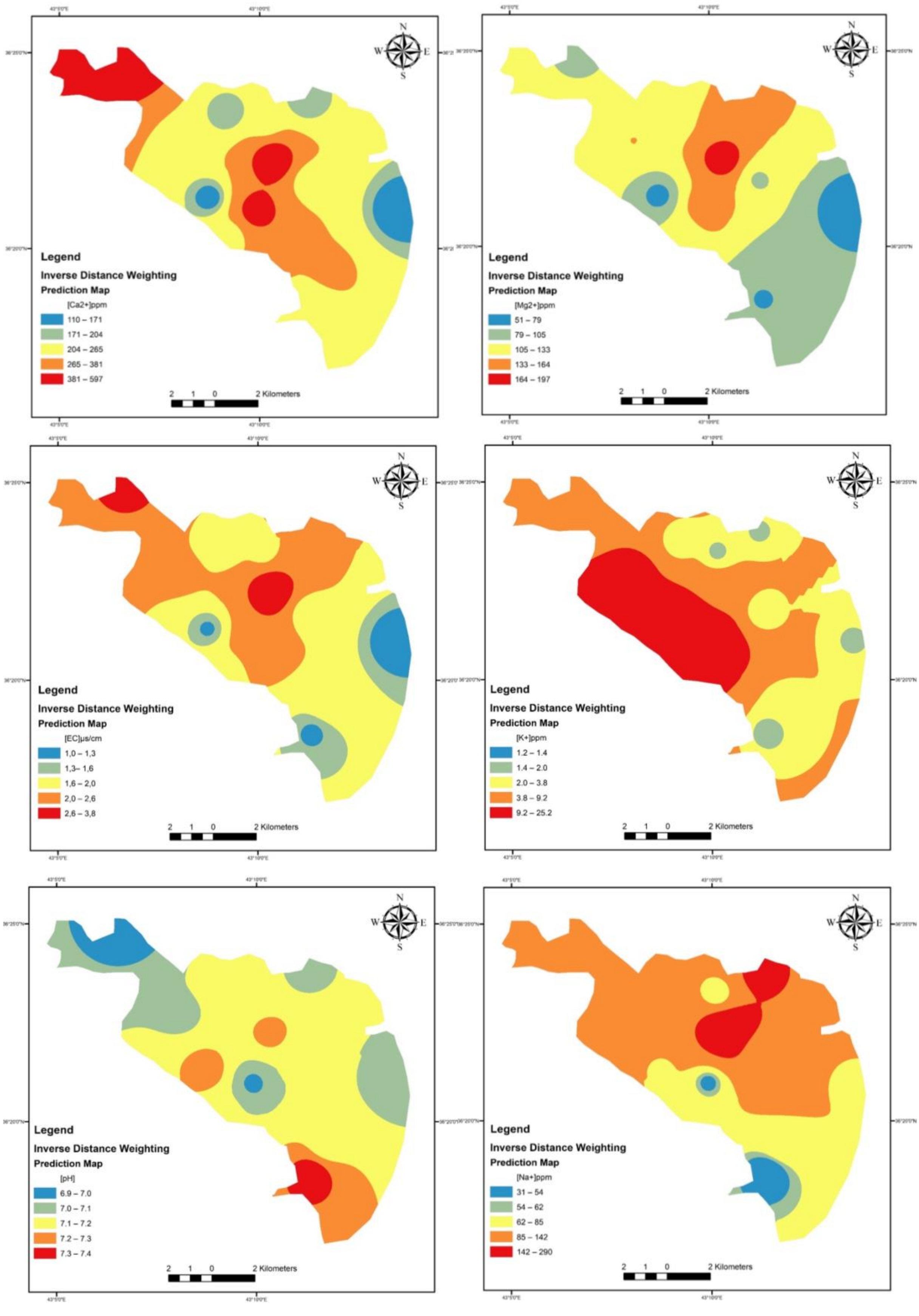


**Fig.2**. Spatial distribution model of groundwater quality parameters for left bank of Mosul city.

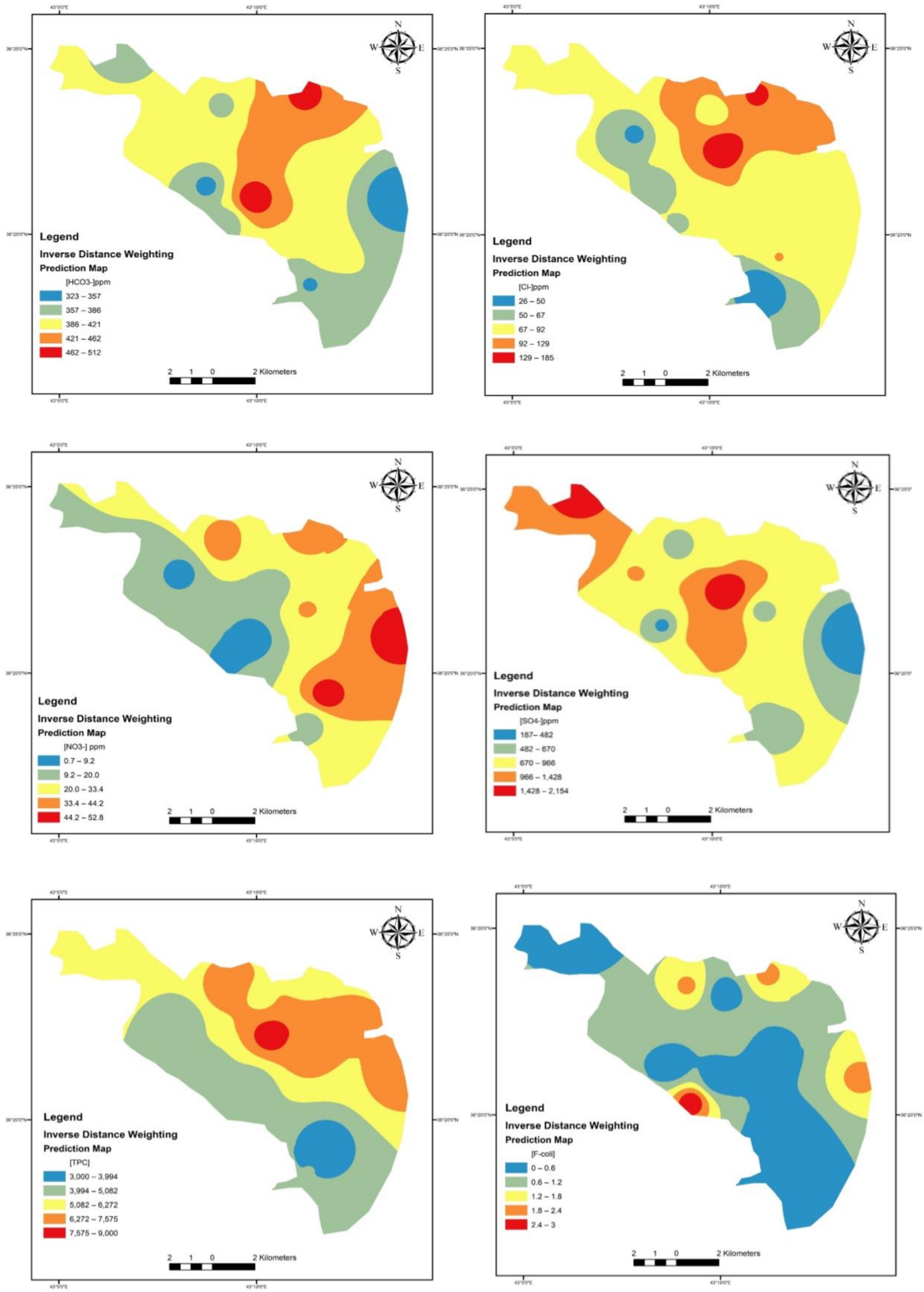


Fig.2 (continued)

## 4. Conclusions

- The spatial model findings suggest that the groundwater on the eastern side of Mosul is polluted by septic tanks and the sewage system. It also revealed that carbonite and evaporite rocks have the greatest influence on groundwater hydrochemistry in the study area. Furthermore, the groundwater in the left side of Mosul City has higher values for most water quality parameters.
- The current spatial models of water quality parameters can help authorities and planners make informed decisions about the best future locations for drilling wells and their suitability for various uses.
- The present study demonstrated the effectiveness of GIS in providing information on groundwater quality, which aids in the study and evaluation of the state of water by representing water quality characteristics in the form of maps that display water quality information in a simplified manner.

## References


Adnan, S. and Iqbal, J., 2014. Spatial analysis of the groundwater quality in the Peshawar District, Pakistan, Procedia Engineering, 70, 14–22.

Al-Jiburi, H. K. and Al-Basrawi, N. H.,2015. Hydrogeological map of Iraq, scale 1: 1000 000, 2nd EDITION, 2013, Iraqi Bulletin of Geology and Mining, 11(1), 17 − 26.

APHA, 2005. Standard methods for the examination of water and waste water. 21st ed. Washington, D.C: American Public Health Association.

AtlasWorld, 2019. Where Is Mosul, Iraq?

Barmakova, D. B. et al., 2022. Spatial analysis of the chemical regime of groundwater in the karatal irrigation Massif in South-Eastern Kazakhstan, Water Multidisciplinary Digital Publishing Institute, 14(3), 285.

Climate-Data.Org, 2019. Climatemosul, 1248

Dandge, K. P. and Patil, S. S.,2021. Spatial distribution of ground water quality index using remote sensing and GIS techniques, Applied Water Science, 12(1), 7.

Ditthakit, P. et al., 2021. Estimating baseflow and baseflow index in ungauged basins using spatial interpolation techniques: A case study of the Southern River Basin of Thailand', Water, 13, 3113.

Guinea, A. et al., 2012.The electrical properties of calcium sulfate rocks from decametric to micrometric scale', Journal of Applied Geophysics, 85, 80–91.

Kale, A. et al., 2020.Factor analysis and spatial distribution of water quality parameters of Aurangabad District, India, Groundwater for Sustainable Development, 10.

Khattab, M. F. O. et al. 2020. Variable reduction for water quality investigation using VARCLUS Technique. A case study of Mosul Dam Lake, Northern Iraq', Water Resources, 47(6), 1005–1011.

Khattab, M. F. O. et al.,2021.Water quality investigation of recent wells which were randomly dug at the left side of Mosul City, Advances in Science, Technology and Innovation. Springer, Cham, 297–306.

Khattab, M. F. O. and Merkel, B.,2015. Secchi disc visibility and its relationship with water quality parameters in the photosynthesis zone of Mosul Dam Lake, Northern Iraq', FOG - Freiberg Online Geoscience, 39.

Khattab, M. F. O. and Merkel, B. J., 2012. Distribution of heterotrophic bacteria and water quality parameters of Mosul Dam Lake, Northern Iraq', WIT Transactions on Ecology and the Environment, 164.

Liu, Z., Xu, B., Cheng, B. and Hu, X., 2021. Interpolation parameters in inverse distance-weighted interpolation algorithm on DEM interpolation error. Journal of Sensors, 2021, 1-14.

Pande, C. B. and Moharir, K., 2018. Spatial analysis of groundwater quality mapping in hard rock area in the Akola and Buldhana districts of Maharashtra, India', Applied Water Science, 8(4), 106.

Panno, S. et al., 2006. Characterization and Identification of Na-Cl Sources in Ground Water, Ground water, 44, 176–187.

Saha, S., Reza, A. H. M. S. and Roy, M. K., 2019, Hydrochemical evaluation of groundwater quality of the Tista floodplain, Rangpur, Bangladesh, Applied Water Science, 9(8), 198.

Saleh, D. K.,2010. Stream Gage Descriptions and Streamflow Statistics for Sites in the Tigris River and Euphrates River Basins, Iraq.

Satyaji Rao, Y., Keshari, A. K. and Gosain, A.,2012. Nitrate leaching estimation from faulty septic tank using RISK-N Model, J. Applied Hydrology, XXV, 9–27.

Sissakian, V. K., 1995. The Geology of Al-Mosul Quadrangle sheet NJ-38-3 (GM 4) scale 1:250 000. Baghdad.

Sundaram, B., 2009. Groundwater Sampling and Analysis – A Field Guide'.

UN-Habitat, 2016. City Profile Of Mosul, Iraq.Multi-sector assessment of a city under siege.

WeatherSpark, 2019.Average Weather in Mosul.

Zhang, B., Zhao, D., Zhou, P., Qu, S., Liao, F. and Wang, G., 2020. Hydrochemical characteristics of groundwater and dominant water–rock interactions in the Delingha Area, Qaidam Basin, Northwest China. Water, 12(3), 836.

Zhou, Q. and Li, J.,2020. Geo-Spatial Analysis in Hydrology, ISPRS International Journal of Geo-Information, 9(7). doi: 10.3390/ijgi9070435.